

# 1     **Transport formula for collisional sheet flows with turbulent suspension**

2                                     Diego Berzi<sup>1</sup>

3     <sup>1</sup> Assistant professor, Dept. of Environmental, Hydraulic, Infrastructure, and Surveying Engineering, Politecnico  
4     di Milano, Milan, 20133, Italy. Email: [diego.berzi@polimi.it](mailto:diego.berzi@polimi.it)

## 6     **Abstract**

7     The prediction of the transport of sediments in streams is of crucial importance for many  
8     geophysical and industrial applications. Most of the available formulas for sediment transport  
9     are empirical, and apply to situations near initiation, where a few erratic particles are seen  
10    jumping and rolling over an immobile bed. Yet, they are commonly adopted for predicting  
11    massive transport of sediments, although more rigorous approaches exist. The latter make use  
12    of constitutive relations from kinetic theories of granular gases, but require the numerical  
13    integrations of complicated, non-linear differential equations; hence, discouraging people  
14    from their usage for practical purposes. Here, we propose a new explicit formula for  
15    predicting intense sediment transport that is based on kinetic theories of granular gases and  
16    incorporates in a simple, yet rigorous, way the possibility of turbulent suspension of the  
17    particles. We then show that our formula, unlike others, can quantitatively reproduce physical  
18    experiments on steady, uniform flows of natural and artificial particles and water over  
19    horizontal, movable beds taken from the literature. Our findings suggest that granular physics  
20    is now mature enough to provide practical tools in fields that were so far mainly empirically-  
21    oriented.

22

## 23 **Introduction and theory**

24 Most of researches on sediment transport has put an emphasis on the forces that the liquid  
25 component exerts on the particles, rather than on the particle-particle interactions. This is  
26 partially due to the fact that the laboratory experiments were mostly conducted, for practical  
27 reasons, at small values of water discharge, close to the inception of particle motion, where  
28 inter-particle forces are negligible. At higher values of water discharge, massive transport of  
29 sediments takes instead place, and those forces cannot be ignored. Sophisticated  
30 mathematical models, that take into account the turbulence of the liquid, the inter-particle  
31 collisions, the turbulent suspension and the mutual influence between turbulence and particle  
32 velocity fluctuations have been proposed (Jenkins and Hanes 1998; Hsu et al. 2004). They  
33 require though the numerical solutions of sets of rather complicated differential equations, for  
34 which end-users oriented codes are not available yet; this limits their appeal to audience  
35 interested in practical applications.

36 As recently suggested (Frey and Church 2009), we use up to date findings on granular  
37 physics to provide a simple description of intense sediment transport, here defined as the  
38 massive flow of particles dominated by collisional exchange of momentum (i.e., Shields  
39 numbers higher than about four times the critical value at the inception of particle motion; see  
40 later in the text), possibly in presence of turbulent suspension. We focus, for simplicity, on  
41 the case of the transport of uniform, rigid spheres of diameter  $d$  immersed in water (with  $\rho$   
42 and  $\eta$  the water density and viscosity, respectively, and  $\sigma$  the ratio of particle to water  
43 density) over a horizontal, plane, movable bed. The shear stress,  $S^*$ , exerted by the water at  
44 the top of the sediments (actually, at the top of the diffuse collisional layer; see later for more  
45 details) represents the driving force of particle motion. It is evident from experiments, that the  
46 volume concentration,  $v$ , of the particles increases towards the bed, while both the time-

47 averaged velocity and the velocity fluctuations of the particles decrease (Sumer et al. 1996;  
48 Armanini et al. 2005; Capart and Fraccarollo 2011).

49 Let us analyze, for the moment, the simpler case of dry granular flows over inclined, movable  
50 beds. Particle-particle interactions can be divided into nearly instantaneous collisions and  
51 enduring contacts (Berzi et al. 2011), with the former dominant at low to moderate  
52 concentrations. For sake of simplicity, but with sufficient accuracy, let us consider that the  
53 influence of enduring contacts is almost entirely captured by the presence of a yielding value  
54 for the ratio of shear to normal stress (the Coulomb criterion). It is customary to characterize  
55 the collisions through a coefficient of restitution, which represents the ratio of pre- to post-  
56 collisional relative velocity between two colliding particles, and assume that it is constant  
57 (Goldhirsch 2003). Inclined, dry granular flows are characterized by the presence at the top of  
58 a ballistic layer, where the mean free path between two consecutive collisions is longer than  
59 the ballistic trajectory that every particle follows under the influence of gravity (Pasini and  
60 Jenkins 2005). This means that one cannot disregard the influence of external forces – in this  
61 case gravity – on the dynamics of particle-particle encounters, and the constitutive relations  
62 provided by kinetic theories of granular gases (Jenkins and Savage 1983; Garzo and Dufty  
63 1999) do not apply. When the mean free path diminishes, due to increasing in particle  
64 concentration, and is less than the length of the ballistic trajectory, kinetic theories of granular  
65 gases are able to provide a correct description of the flow (Goldhirsch 2003). In particular,  
66 when the fluctuating velocities of the particles are uncorrelated, classic kinetic theories apply  
67 (Garzo and Dufty 1999). Berzi and Jenkins (2011) named this region the diffuse collisional  
68 layer. When the concentration further increases – say greater than 0.49 for spheres (Jenkins  
69 2007) – the particle fluctuating velocities are no longer uncorrelated (Kumaran 2009) and one  
70 has to modify the classic kinetic theories to account for the diminished energy dissipation in  
71 collisions (Mitarai and Nakanishi 2007; Jenkins 2006, 2007). This region is called the dense

72 algebraic layer in Berzi and Jenkins (2011). Below the dense algebraic layer, there is the  
73 movable bed, where the ratio of particle shear to normal stress is equal or below the threshold  
74 for having motion.

75 Let us see now how the picture changes in presence of water. At the macroscopic scale, one  
76 has to take into account the particle-water interactions (mainly drag, lift and buoyancy) in the  
77 momentum equations for the particles, but this does not alter the above mentioned layered  
78 structure of the flow. At the microscopic scale, though, the presence of the viscous fluid  
79 damps the collisions. Hence, the value of the coefficient of restitution is no longer constant,  
80 but is a well defined monotonic function of the particle Stokes number  $St$ , i.e., the ratio of  
81 particle inertia to fluid viscous forces: it decreases when the Stokes number decreases (Joseph  
82 et al. 2001). The subsequent layered structure of sediments is represented in Fig. 1, together  
83 with a generic concentration profile. At the top, there is still the presence of a ballistic layer,  
84 although in this case the external forces that cannot be disregarded in describing the dynamics  
85 of particle-particle encounters are the drag force and the buoyancy, in addition to gravity.  
86 Below this, the diffuse collisional and dense algebraic layers are both characterized by the  
87 fact that the coefficient of restitution decreases towards the bed, given that the Stokes number  
88 is proportional to the square root of the granular temperature,  $T$  – the measure of the intensity  
89 of particle velocity fluctuations, the analog at the particle scale of the thermodynamic  
90 temperature of classic gases – that decreases approaching the bed (Armanini et al. 2005;  
91 Berzi 2011). At a certain distance  $\delta$  from the bed, the Stokes number is so low that the  
92 coefficient of restitution vanishes; there, the collisions are perfectly inelastic, and the mixture  
93 of sediment and water behaves as a viscous dense suspension, with an effective viscosity that  
94 depends on the concentration (Boyer et al. 2011). This is the macro-viscous layer (Berzi  
95 2011), just above the movable bed (Fig. 1). Not all the above described layers are always  
96 present in the flow. As shown by Berzi (2011), for values of  $S^*$  lower than a certain value, the

97 dense algebraic layer vanishes; on the other hand, for values of  $S^*$  greater than another  
98 particular value, the macro-viscous layer disappears. Also, we emphasize that the massive  
99 transport of sediments is localized in the diffuse collisional, dense algebraic and macro-  
100 viscous layers, so that the additional contribution of the ballistic layer is usually negligible.  
101 This is not true, though, at the lowest values of  $S^*$  (see later) when the massive transport  
102 layers vanish; in that case, the sediment transport is concentrated in the ballistic layer.  
103 On the basis of the above described physical picture, we were able to obtain an analytical  
104 solution of steady, uniform transport of sediment that applies when the massive transport  
105 layers are present, but the particles are not yet suspended by turbulence (Berzi 2011). This  
106 means that the total depth  $h$  of the massive transport layers, whose expression is reported in  
107 Table 1, must be greater than one diameter, and the ratio of the fluid shear velocity at  $y = h$ ,  
108  $(S^* / \rho)^{1/2}$ , to the uniform settling velocity of a single particle,  $w_0$ , must be less than or equal  
109 to one (Jenkins and Hanes 1998). The transport formula – i.e., the particle volume flow rate  
110 per unit width,  $q$ , as a function of the fluid shear stress  $S^*$  – obtained by extending the work of  
111 Berzi (2011) to deal with turbulent suspension, in the limit of small values of the coefficient  
112 of collisional restitution at  $y = H$ , i.e., at the top of the dense algebraic layer (Fig. 1) – can be  
113 written as:

$$114 \quad \Phi = \psi \theta_{eff}^{3/2}, \tag{1}$$

115 where  $\Phi = q / [g(\sigma - 1)]^{1/2} d^{3/2}$  is the dimensionless particle volume flow rate per unit width;  
116  $\theta_{eff}$  is an effective Shields number (see later), which represents a percentage of the actual  
117 Shields number,  $\theta = S^* / \rho g (\sigma - 1) d$ , i.e., the dimensionless fluid shear stress at the top of the  
118 massive layers;  $g$  is the gravitational acceleration; and the coefficient  $\psi$  is an explicit function  
119 of  $\theta_{eff}$  and the set of particle properties (Table 1). The latter includes the coefficient of  
120 collisional restitution in absence of water,  $\varepsilon$ ; the parameter  $c$  in the expression for the particle

121 velocity correlation in the dense algebraic layer (Jenkins 2006, 2007); the ratio of particle to  
122 liquid density,  $\sigma$ ; the particle Reynolds number,  $R = \rho d [gd(\sigma - 1)/\sigma]^{1/2} / \eta$ , that explicitly  
123 depends on the particle diameter; the approximately constant value of the concentration in the  
124 dense algebraic and macro-viscous layers,  $\bar{v}$ ; and the yielding value of the particle stress  
125 ratio at the bed,  $\alpha$ . All the particle properties have clear physical meanings and can be easily  
126 measured, but for the parameter  $c$ , that must be inferred from experiments; nonetheless,  $c$  is  
127 of order unity and values appropriated for sand, plastic cylinders and glass spheres have been  
128 previously determined (Jenkins and Berzi 2010; Berzi 2011). The dependence of  $\psi$  on the  
129 effective Shields number for natural sand or gravel of different diameters (equivalently, for  
130 different value of the particle Reynolds number) in water is plotted in Fig. 2; as in Berzi  
131 (2011), we employ the following values for the particle properties:  $\varepsilon=0.45$ ,  $c=0.65$ ,  
132  $\sigma=2.67$ ,  $\bar{v}=0.65$  and  $\alpha=0.50$ . For diameters greater than 10 mm, corresponding to particle  
133 Reynolds numbers greater than 2500, the curves collapse onto a single one. It is worth  
134 noticing that the most used formulas for sediment transport, such as the famous one proposed  
135 by Meyer-Peter and Müller (1948) – MPM formula, from now on –, and its revised form  
136 proposed by Wong and Parker (2006) – WP formula –, but also the recent, physically-  
137 sounded formula of Capart and Fraccarollo (2011) – CF formula – are characterized by a  
138 coefficient of proportionality of  $\Phi$  with the Shields number to the power of  $3/2$ , independent  
139 on both the Shields number, at least far from the inception of particle motion, and the  
140 properties of the particles. The literature constant values of the coefficient of proportionality  
141 are 8 (MPM formula) and around 4 (WP and CF formulas), while Fig. 2 shows a much wider  
142 interval of variation for  $\psi$ .

143 We introduced the effective Shields number in Eq.(1) motivated by the work of McTigue  
144 (1981), where a rigorous analysis of the influence of the turbulence on the particles in a  
145 mixture resulted in an additional term proportional to the gradient of concentration that must

146 be included in the particle momentum balances (see also Hsu et al. 2004). With this, the  
 147 particle momentum balance in the vertical direction reads

$$148 \quad p' = -v\rho(\sigma-1)g - C \frac{\eta_T}{\rho} v', \quad (2)$$

149 with  $p$  particle pressure,  $C$  drag coefficient and  $\eta_T$  turbulent viscosity. The prime indicates the  
 150 spatial derivative along the vertical direction. We assume that the drag coefficient can be  
 151 expressed in terms of the uniform settling velocity  $w$  of particles at concentration  $v$ , provided  
 152 that, at equilibrium (i.e., when the drag force is balanced by the buoyant weight),

$$153 \quad Cw = v\rho(\sigma-1)g. \quad (3)$$

154 Both  $\eta_T$  and  $w$  are local quantities. However, we can assume that, on average, they are  
 155 proportional to  $(\rho S^*)^{1/2} (h-H)$  (McTigue 1981) and  $w_0$ , respectively. Then, taking  $v$  to be  
 156 approximately linearly distributed from 0, at the top, to  $\bar{v}$ , at  $y = H$ ,

$$157 \quad p' = -\rho(\sigma-1)vg \left[ 1 - \bar{v}\xi \frac{(S^*/\rho)^{1/2}}{w_0} \right]. \quad (4)$$

158 where  $\xi$  is a coefficient of order unity. Eq. (4) shows that the collisional pressure decreases  
 159 when the turbulent suspension is present. The analytical solution resulting in Eq.(1) and  
 160 Table 1 is based on the determination of the ratio of particle shear stress to particle pressure  
 161 in the dense layers of Fig. 1 (dense algebraic and macro-viscous layer). There, the  
 162 dimensionless particle shear stress equals the Shields number, because the turbulence is likely  
 163 to be suppressed (Berzi 2011). Hence, decreasing the particle pressure by the factor of Eq. (4)  
 164 is equivalent to increasing the Shields number by the inverse of the same factor. We therefore  
 165 introduce the effective Shields number as

$$166 \quad \frac{\theta_{eff}}{1 + \bar{v}\xi - \bar{v}\xi \left[ \theta_{eff} g (\sigma-1) d \right]^{1/2} / w_0} = \theta. \quad (5)$$

167 The factor in Eq.(5) has been slightly modified with respect to that in Eq.(4) to ensure that  $\theta_{eff}$   
168 coincides with  $\theta$  for  $(S^* / \rho)^{1/2}$  equal to  $w_0$  (i.e., when the turbulent suspension vanishes in  
169 the diffuse collisional layer).

170 As already mentioned, the minimum Shields number for which the transport formula (1)  
171 holds is that for which the depth of the massive transport layers is at least one diameter. From  
172 Table 1, and the idea that at such low values of the Shields number the coefficient of  
173 collisional restitution at the top of the dense layers  $e_H$  approximately vanishes (Berzi 2011),  
174 as well as the turbulent suspension, this implies  $\theta > \alpha \bar{v} / (1.22\alpha + 1)$ . For sand, this minimum  
175 value is roughly 0.2, i.e., about four times the critical value for the inception of motion. On  
176 the other hand, the maximum value of the actual Shields number for the validity of Eq.(1) is  
177 that for which the turbulent suspension is so strong that the collisional pressure at the top of  
178 the dense layers vanishes (inception of fully suspended load). Hence, from Eq.(4),  
179  $\theta < w_0^2 / [\bar{v}^2 \xi^2 g (\sigma - 1) d]$ .

## 180 **Comparison with experiments and conclusions**

181 We now test Eq.(1) against the experimental results reported by Nnadi and Wilson (1992) on  
182 the flows of 0.7 mm sand in water (Fig. 3). Those experiments possess some unique features  
183 that make them perfect to test sediment transport formulas: (i) they have been performed with  
184 natural material, hence satisfying those skeptical about the use of unrealistic artificial  
185 particles in laboratory experiments; (ii) they have been obtained on horizontal, plane movable  
186 bed, so that additional complications such as gravity in the flow direction and bedforms  
187 (Wong and Parker 2006) are ruled out; (iii) the experimentally investigated values of the  
188 Shields number, in the interval between 0.8 and 8, pretty much cover the range of most



189 interest for practical applications in Hydraulics (for instance, they are associated with the  
190 intense sediment transport occurring during floods).

191 The turbulent suspension is not expected to play a role for  $\theta \leq 1$ , given that the single  
192 particle, uniform settling velocity for 0.7 mm sand is about 10 cm/s (Abrahams 2003).  
193 Indeed, Fig.3 shows that Eq. (1) without turbulent suspension, i.e., with  $\theta_{eff} = \theta$ , reproduces  
194 the experiments up to a value of the Shields number slightly above one, while over-predicts  
195 the transport rate for larger values of  $\theta$ . When we use Eq.(5) to evaluate  $\theta_{eff}$ , with  $\xi$  equal to  
196 0.6, the quantitative agreement of Eq.(1) with the experiments is remarkable (Fig. 3), even at  
197 values of  $\theta$  slightly greater than that for which Eq.(1) is valid (about 6.5 in the case of  
198 0.7 mm sand). Transport formulas other than Eq.(1) constantly under-predict the  
199 experimental data (Fig. 3); the better performance of the MPM formula with respect to both  
200 WP and CF expressions is likely to be fortuitous, given that the analysis of Wong and Parker  
201 (2006) proved that it was based on erroneous interpretation of the experimental results.

202 Fig. 4 shows the comparison between measured (Nnadi and Wilson 1992) and predicted  
203 values of dimensionless particle flow rate per unit width of artificial particles and water. The  
204 experiments were performed using mono-dispersed Bakelite beads of two different diameters  
205 and water. This allows to investigate the role of the particle Reynolds number on the particle  
206 transport rate; with  $\sigma = 1.56$ ,  $R = 46$  and  $64$ , when  $d = 0.67$  and  $1$  mm, respectively. To plot  
207 the theoretical curves of Fig. 4, we have employed  $\varepsilon=0.6$ ,  $c=0.5$ ,  $\bar{v}=0.55$  and  $\alpha=0.50$ , as  
208 appropriated for PVC particles (Berzi 2011);  $\xi = 0.6$ , as for sand, and  $w_0$  equal to  $7$  cm/s  
209 (Ferguson and Church 2004). As predicted by the theory (Berzi 2011), at lower values of the  
210 Reynolds number correspond higher values of  $\Phi$ , for a given Shields number (Fig.4). Once  
211 again, the agreement between the transport formula (1) and the experiments is notable.

212 We conclude that the proposed formula for predicting intense sediment transport is simple  
213 enough to be used for practical purposes, yet rigorous enough, being based on kinetic

214 theories, and granular physics in general, that there is no need for additional tuning  
215 parameters; it also has a superior capability of reproducing experiments. The limits of the  
216 approach regard, as already mentioned, the prediction of the sediment transport at (i) Shields  
217 numbers close to the inception of particle motion (say less than four times the critical value),  
218 for which the constitutive relations of kinetic theories do not apply; (ii) Shields numbers  
219 larger than the inception of fully suspended sediment transport, at which the collisional  
220 pressure vanishes (about 7 for 0.7 mm sand).

## 221 **Notation**

222 *The following symbols are used in the paper:*

223

224  $c$  = parameter in the expression for the particle velocity correlation;

225  $C$  = drag coefficient;

226  $d$  = particle diameter;

227  $e_H$  = coefficient of collisional restitution at the top of the dense algebraic layer;

228  $g$  = gravitational acceleration;

229  $h$  = total depth of the diffuse collisional, dense algebraic and macro-viscous layers;

230  $H$  = total depth of the dense algebraic and macro-viscous layers;

231  $k$  = particle stress ratio at the top of the dense algebraic layer;

232  $p$  = particle pressure;

233  $q$  = particle volume flow rate per unit width;

234  $R$  = particle Reynolds number;

235  $S^*$  = water shear stress at the top of the diffuse collisional layer;

236  $St$  = Stokes number;

237  $T$  = granular temperature;

238  $w$  = uniform settling velocity of particles at concentration  $v$ ;

239  $w_0$  = uniform settling velocity of a single particle;  
240  $x$  = coordinate in the flow direction;  
241  $y$  = coordinate in the direction perpendicular to the bed;  
242  $\alpha$  = yielding value of the stress ratio at the bed;  
243  $\delta$  = depth of the macro-viscous layer;  
244  $\varepsilon$  = coefficient of collisional restitution in dry conditions;  
245  $\Phi$  = dimensionless particle volume flow rate per unit width;  
246  $\eta$  = molecular viscosity;  
247  $\eta_T$  = turbulent viscosity;  
248  $\lambda$  = particle stress ratio at the top of the macro-viscous layer;  
249  $v$  = concentration;  
250  $\bar{v}$  = approximately constant concentration in the dense layers;  
251  $\theta$  = Shields number;  
252  $\theta_{eff}$  = effective Shields number;  
253  $\rho$  = water density;  
254  $\sigma$  = particle density over water density;  
255  $\xi$  = material coefficient;  
256  $\psi$  = coefficient in the transport formula;  
257  $\psi_i$  = auxiliary coefficient (with  $i = 1, 2, 3$ ).

## 258 **References**

259 Abrahams, A.D. (2003). "Bed-Load Transport Equation for Sheet Flow." *J. Hydraul. Eng.-ASCE*,  
260 129(2), 159–163.  
261 Armanini, A., Capart, H., Fraccarollo, L., and Larcher, M. (2005). "Rheological stratification in  
262 experimental free-surface flows of granular-liquid mixtures." *J. Fluid Mech.*, 532, 269–319.

263 Berzi, D. (2011). “Analytical Solution of Collisional Sheet Flows.” *J. Hydraul. Eng.-ASCE*, 137(10),  
264 1200–1207.

265 Berzi, D., Di Prisco, C.G., and Vescovi, D. (2011). “Constitutive relations for steady, dense granular  
266 flows.” *Phys. Rev. E*, 84(3), 031301.

267 Berzi, D., and Jenkins, J.T. (2011). “Surface Flows of Inelastic Spheres.” *Phys. Fluids*, 23, 013303.

268 Boyer, F., Guazzelli, E., and Pouliquen, O. (2011). “Unifying Suspension and Granular Rheology.”,  
269 *Phys. Rev. Lett.*, 107, 188301.

270 Capart, H., and Fraccarollo, L. (2011). “Transport layer structure in intense bed-load.” *Geophys. Res.*  
271 *Lett.*, 38, L20402.

272 Ferguson, R.I., and Church, M. (2004). “A Simple Universal Equation for Grain Settling Velocity.” *J.*  
273 *Sediment. Res.*, 74, 933–937.

274 Frey, P. and Church, M. (2009). “How river beds move.” *Science*, 325, 1509–1510.

275 Garzo, V., and Dufty, J.W. (1999). “Dense fluid transport for inelastic hard spheres.” *Phys. Rev. E*,  
276 59, 5895.

277 Goldhirsch, I. (2003). “Rapid granular flows.” *Ann. Rev. Fluid Mech.*, 35, 267–293.

278 Hsu, T.-J., Jenkins, J.T., and Liu, P. L.-F. (2004). “On two-phase sediment transport: sheet flow of  
279 massive particles.” *Proc. R. Soc. A-Math. Phys. Eng. Sci.*, 460, 2223–2250.

280 Jenkins, J.T. (2006). “Dense shearing flows of inelastic disks.” *Phys. Fluids*, 18, 103307.

281 Jenkins, J.T. (2007). “Dense inclined flows of inelastic spheres.” *Gran. Matt.*, 10, 47–52.

282 Jenkins, J.T., and Berzi, D. (2010). “Dense Inclined Flows of Inelastic Spheres: Tests of an Extension  
283 of Kinetic Theory.” *Gran. Matt.*, 12, 151–158.

284 Jenkins, J.T., and Hanes, D.M. (1998). “Collisional sheet flows of sediment driven by a turbulent  
285 fluid.” *J. Fluid Mech.*, 370, 29–52.

286 Jenkins, J.T., and Savage, S.B. (1983). “A theory for the rapid flow of identical, smooth, nearly elastic  
287 particles.” *J. Fluid Mech.*, 130, 187–202.

288 Joseph, G.G., Zenit, R., Hunt, M.L., and Rosenwinkel, A.M. (2001). “Particle-wall collisions in a  
289 viscous fluid.” *J. Fluid Mech.*, 433, 329–346.

290 Kumaran, V. (2009). "Dynamics of dense sheared granular flows. Part II. The relative velocity  
291 distributions." *J. Fluid. Mech.*, 632, 145–198.

292 McTigue, D.F. (1981). "Mixture Theory for Suspended Sediment Transport." *J. Hydraul. Div.*, 107,  
293 659–673.

294 Meyer-Peter, P., and Müller, R. (1948). "Formulas of bed-load transport." *Proc. 2nd Congress IAHR*,  
295 (Int. Association for Hydr. Res.), Stockholm, Sweden.

296 Mitarai, N., and Nakanishi, H. (2007). "Velocity correlations in dense granular shear flows: Effects on  
297 energy dissipation and normal stress." *Phys. Rev. E*, 75, 031305.

298 Nnadi, F.N., and Wilson, K.C. (1992). "Motion of Contact-Load Particles at High Shear Stress.", *J.*  
299 *Hydraul. Eng.-ASCE*, 118(12), 1670–1684.

300 Pasini, J.M., and Jenkins, J.T. (2005). "Aeolian transport with collisional suspension." *Phil. Trans. R.*  
301 *Soc. A*, 363, 1625–1646.

302 Sumer, B.M., Kozakiewicz, A., Fredsoe, J., and Deigaard, R. (1996). "Velocity and concentration  
303 profiles in sheet-flow layer of movable bed." *J. Hydraul. Eng.-ASCE*, 122(10), 549–558.

304 Wong, M., and Parker, G. (2006). "Reanalysis and Correction of Bed-Load Relation of Meyer-Peter  
305 and Müller Using Their Own Database." *J. Hydraul. Eng.-ASCE*, 132, 1159–1168.

## List of tables

**Table 1.** Summary of the analytical results obtained from the theory of Berzi (2011).

Analytical expression	Definition
$\Psi = \Psi_1 \theta_{eff}^{1/2} + \Psi_2 \theta_{eff} + \Psi_3 \theta_{eff}^{3/2}$	Transport coefficient in Eq.(1)
$\Psi_1 = \frac{69(1+\varepsilon)}{\varepsilon \bar{v} \sigma^{3/2} R} \frac{(1+e_H)}{(1-e_H/\varepsilon)(0.44+0.61e_H)} \frac{1}{k}$	Auxiliary coefficient
$\Psi_2 = \frac{0.65c^{1/2}}{\bar{v}^{3/2} \sigma^{1/2}} \frac{1}{(0.44+0.3e_H)^4} \left(\frac{\lambda+k}{2}\right)^{9/2} \left(\frac{1}{\lambda^{3/2}} - \frac{1}{k^{3/2}}\right)$	Auxiliary coefficient
$\Psi_3 = 1400\sigma^{1/2} \bar{v} R c^6 \left(\frac{\alpha+\lambda}{2}\right)^{18} \left(\frac{1}{\alpha^2} - \frac{1}{\lambda^2}\right)$	Auxiliary coefficient
$h = \frac{\theta_{eff}}{\bar{v}} \left(\frac{1}{\alpha} + \frac{1}{k}\right)$	Total depth of the massive transport layers
$k = 1.24 \left[ \frac{(0.44+0.61e_H)(1-e_H)}{1+e_H} \right]^{1/2}$	Ratio of particle shear to normal stress at the top of the algebraic layer
$\lambda = \min \left\{ 1.87 \left[ \frac{\bar{v}(1+\varepsilon)^2}{c^3 \sigma^2 R^2 \varepsilon^2} \right]^{1/8} \theta_{eff}^{-1/8}; 0.82 \right\}$	Ratio of particle shear to normal stress at the top of the macro-viscous layer
$e_H = \varepsilon \max \left\{ \frac{c^{3/2} \varepsilon \sigma R \theta_{eff}^{1/2} - 27 \bar{v}^{1/2} (1+\varepsilon)}{c^{3/2} \varepsilon \sigma R \theta_{eff}^{1/2} + 37 \bar{v}^{1/2} \varepsilon (1+\varepsilon)}; 0 \right\}$	Coefficient of collisional restitution at the top of the dense algebraic layer

Figure 1  
[Click here to download high resolution image](#)

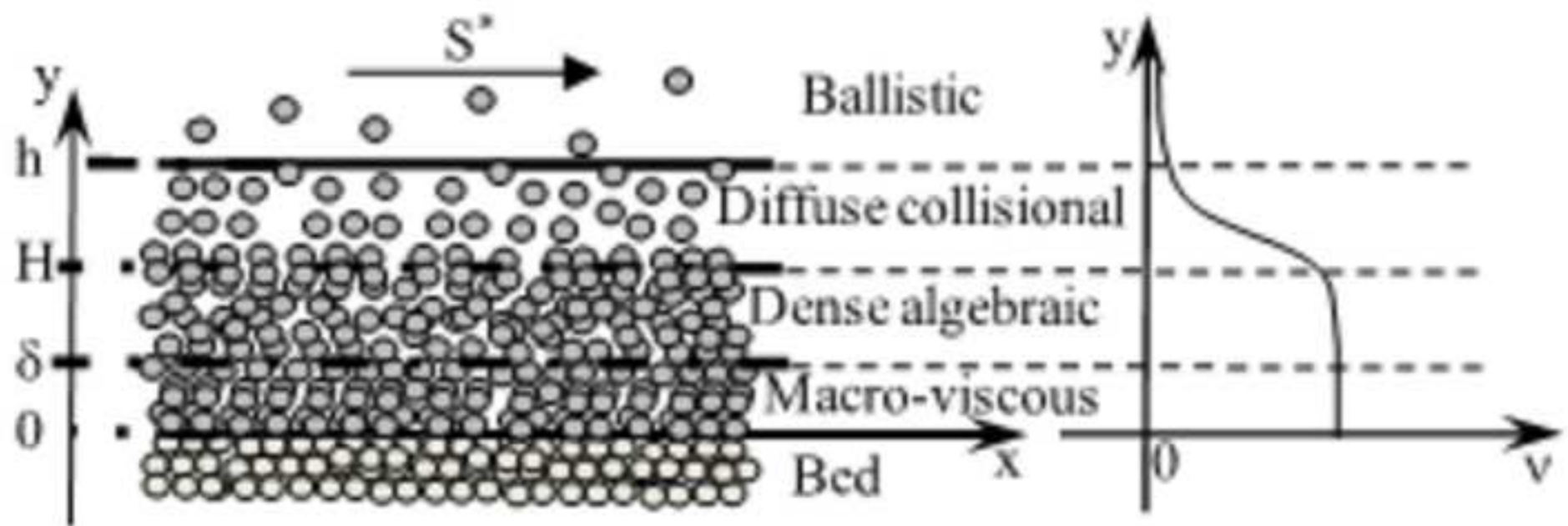


Figure 2  
[Click here to download high resolution image](#)

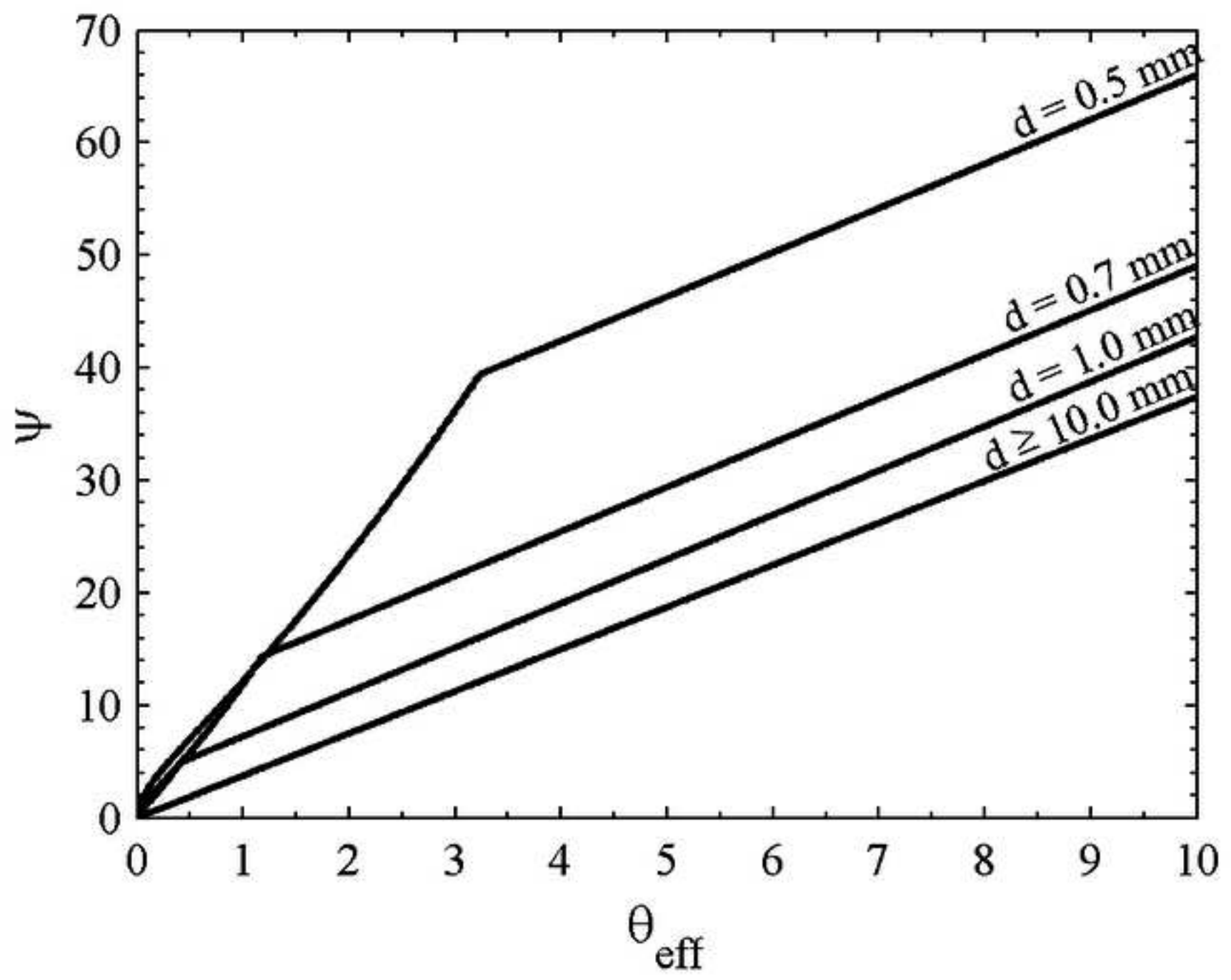




Figure 3  
[Click here to download high resolution image](#)

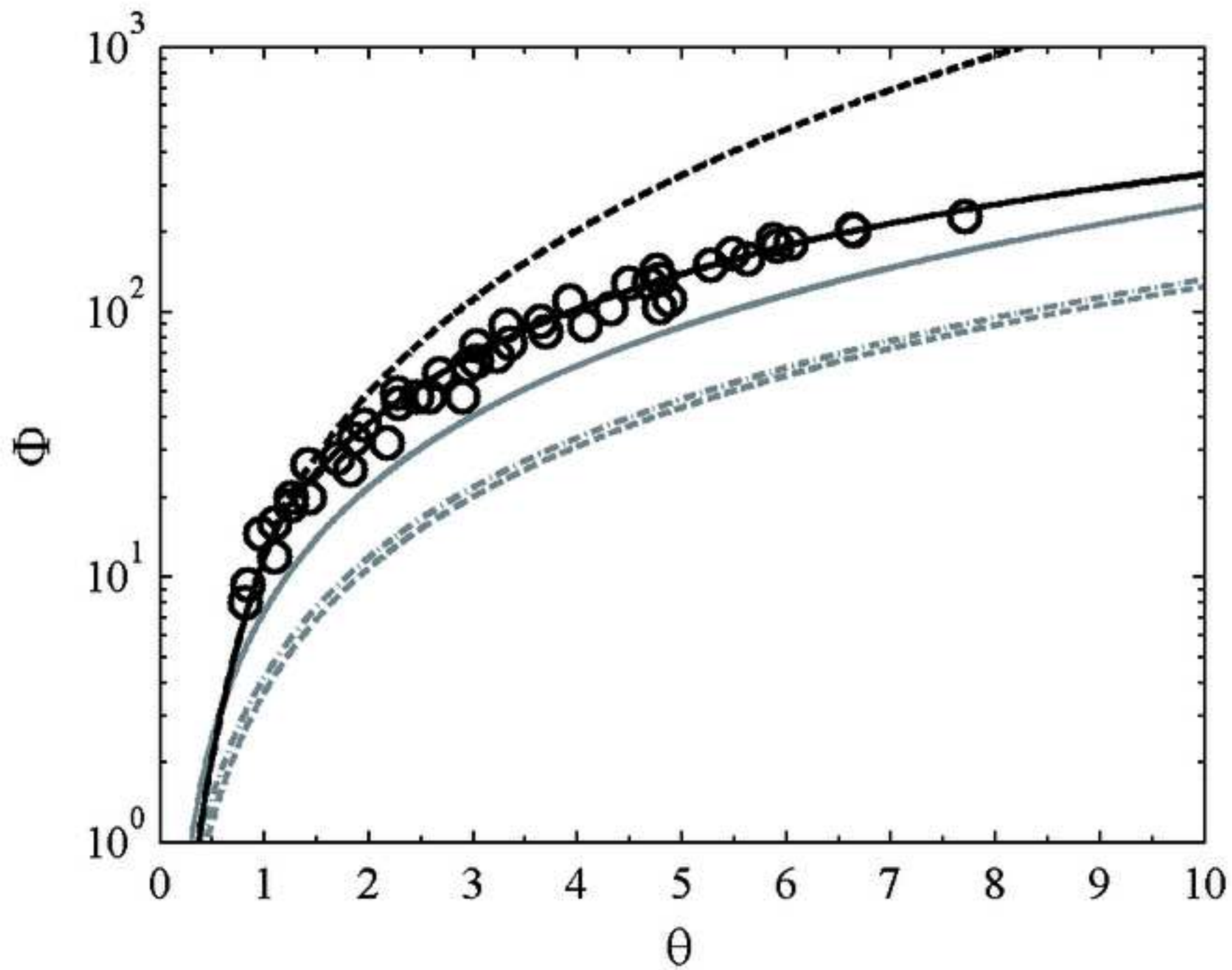
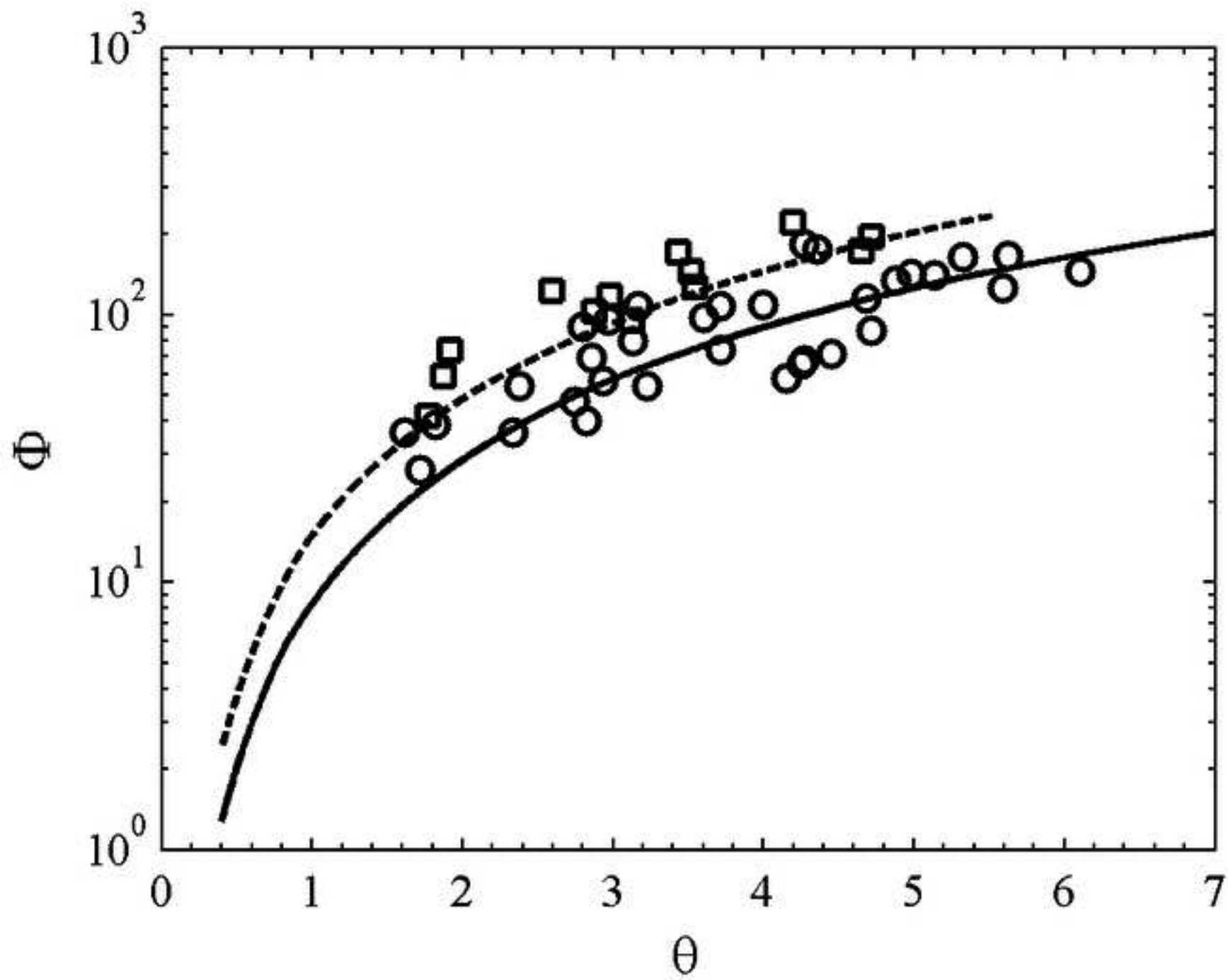


Figure 4  
[Click here to download high resolution image](#)



## List of figure captions

**Figure 1.** Layered structure of sediment transport over a horizontal movable bed and associated concentration profile.

**Figure 2.** Coefficient  $\psi$  of Eq.(1) as function of the effective Shields number for sand/gravel of different diameters in water.

**Figure 3.** Experimental (open circles, after Nnadi and Wilson 1992) data of dimensionless particle volume flow rate per unit width as function of the Shields number for 0.7 mm sand in water. The lines represent the predictions of different formulas for sediment transport: solid black line, Eq.(1); dashed black line, Eq.(1) without including turbulent suspension (i.e.,  $\theta_{eff} = \theta$ ); solid gray line, MPM formula; dot-dashed gray line, WP formula; dashed gray line, CF formula.

**Figure 4.** Experimental (symbols, after Nnadi and Wilson 1992) and theoretical (lines) dimensionless particle volume flow rate per unit width as function of the Shields number for 1 mm (open circles and solid line) and 0.67 mm (open squares and dashed line) Bakelite beads in water.